www.nature.com/labinvest

ARTICLE

Renal denervation ameliorates cardiac metabolic remodeling in diabetic cardiomyopathy rats by suppressing renal SGLT2 expression

Jun-Yu Huo[1,2], Wan-Ying Jiang[1,2], Shi-Geng Zhang[1], Yi-Ting Lyu[1], Jie Geng[1], Meng Chen[1], Yuan-Yuan Chen[1], Zhi-Xin Jiang[1]✉ and Qi-Jun Shan[1]✉

This study aimed to investigate the effects of renal denervation (RDN) on diabetic cardiomyopathy (DCM) and explore the related mechanisms. Male Sprague-Dawley rats were fed high-fat chow and injected with low-dose streptozotocin to establish a DCM model. Six rats served as controls. The surviving rats were divided into three groups: control group, DCM group and DCM + RDN group. RDN surgery was performed in the fifth week. At the end of the experiment, all rats were subjected to ^{18}F-FDG PET/CT and metabolic cage studies. Cardiac function and structure were evaluated by echocardiography and histology. Myocardial substrate metabolism and mitochondrial function were assessed by multiple methods. In the 13th week, the DCM rats exhibited cardiac hypertrophy and interstitial fibrosis accompanied by diastolic dysfunction. RDN ameliorated DCM-induced cardiac dysfunction (E/A ratio: RDN 1.07 ± 0.18 vs. DCM 0.93 ± 0.12, $P < 0.05$; E/E' ratio: RDN 10.74 ± 2.48 vs. DCM 13.25 ± 1.99, $P < 0.05$) and pathological remodeling (collagen volume fraction: RDN 5.05 ± 2.05% vs. DCM 10.62 ± 2.68%, $P < 0.05$). Abnormal myocardial metabolism in DCM rats was characterized by suppressed glucose metabolism and elevated lipid metabolism. RDN increased myocardial glucose uptake and oxidation while reducing the absorption and utilization of fatty acids. Meanwhile, DCM decreased mitochondrial ATP content, depolarized the membrane potential and inhibited the activity of respiratory chain complexes, but RDN attenuated this mitochondrial damage (ATP: RDN 30.98 ± 7.33 μmol/gprot vs. DCM 22.89 ± 5.90 μmol/gprot, $P < 0.05$; complexes I, III and IV activity: RDN vs. DCM, $P < 0.05$). Furthermore, both SGLT2 inhibitor and the combination treatment produced similar effects as RDN alone. Thus, RDN prevented DCM-induced cardiac dysfunction and pathological remodeling, which is related to the improvement of metabolic disorders and mitochondrial dysfunction.

Laboratory Investigation (2022) 102:341–351; https://doi.org/10.1038/s41374-021-00696-1

INTRODUCTION

According to the International Diabetes Federation, diabetes is estimated to cause four million deaths each year worldwide, and this statistic is still increasing at alarming rates[1]. This phenomenon results from not only the continuously increasing prevalence of diabetes[2] but also the high mortality rate caused by diabetes-related complications, especially cardiovascular complications[3]. Among these complications, diabetic cardiomyopathy (DCM) has attracted increasing attention in recent years. DCM, which is caused by hyperglycemia and insulin resistance in the heart, is characterized by ventricular hypertrophy and myocardial fibrosis[4]. This type of cardiovascular complication can result in cardiac diastolic and systolic dysfunction and ultimately promote the development of heart failure, which dramatically increases the mortality of diabetic patients[5]. At present, however, there is no specific treatment for DCM. Thus, any approach to alleviate DCM has the potential to reduce mortality in patients with diabetes.

Although many factors, such as increased oxidative stress[6] and overactive inflammatory pathways[7], are implicated in the pathogenesis of DCM, disrupted substrate utilization and energy metabolism are the underlying causes of these pathological changes and cellular injury[4]. With the development of diabetes, hyperglycemia and insulin resistance suppress myocardial glucose uptake and utilization, leading to the accumulation of advanced glycation end products (AGEs). To maintain the ATP supply, hearts of patients with diabetes rely heavily on free fatty acids (FFAs) as the major substrate for mitochondrial oxidative phosphorylation[8]. However, the imbalance between FFA availability and the oxidation rate leads to the accumulation of triacylglycerol and lipid intermediates in the myocardium[9]. The resulting glucotoxicity and lipotoxicity cause the O-GlcNAcylation of various proteins and uncoupling of mitochondrial oxidative phosphorylation, thus impairing mitochondrial function[10], reducing myocardial efficiency and ATP production[11], and promoting the activation of fibroblasts[12] and apoptosis of cardiomyocytes[13], ultimately leading to cardiac remodeling and dysfunction[8]. Therefore, the regulation of myocardial metabolism may serve as a potential therapeutic target for DCM.

[1]Department of Cardiology, The First Affiliated Hospital of Nanjing Medical University, Nanjing, China. [2]These authors contributed equally: Jun-Yu Huo, Wan-Ying Jiang. ✉email: zhixin_jiang@njmu.edu.cn; qjshan@njmu.edu.cn

Received: 30 July 2021 Revised: 16 October 2021 Accepted: 28 October 2021
Published online: 13 November 2021

Renal denervation (RDN), a new neurohumoral regulation technique[14], can effectively reduce blood pressure, improve cardiac function, and delay cardiac remodeling in many cardiovascular disease models by removing renal sympathetic nerves[15, 16]. In the clinic, RDN is currently used for the treatment of resistant hypertension, which is safe for patients and has long-lasting effects without poor compliance or side effects, such as oral drugs[17]. However, the clinical efficacy of RDN is not always stable due to the complex pathogenesis of hypertension[18]. Nevertheless, recent basic studies hint that RDN might have more indications beyond hypertension. Rafiq *et al*. found that the hyperactivity of renal sympathetic nerves promoted the overexpression of sodium-glucose cotransporter 2 (SGLT2) in renal tubules, thereby promoting urinary glucose reabsorption and increasing the blood glucose level[19]. Meanwhile, clinical trials have proven that inhibition of renal SGLT2 by inhibitors of SGLT2, such as dapagliflozin, can improve glycemic control and alleviate myocardial inflammation and oxidative stress and is therefore used for the treatment of DCM[20, 21]. On this basis, RDN may also play a similar role as SGLT2 inhibitors to reduce the blood glucose concentration by inhibiting renal sympathetic activity[22]. However, the effect of RDN on glucose metabolism in the DCM model remains to be fully elucidated. Therefore, we established a rat DCM model to explore the effect of RDN on the diabetic heart, explained the related mechanisms from the perspective of myocardial energy metabolism, and then compared its effect with that of an SGLT2 inhibitor in DCM rats.

MATERIALS AND METHODS

Animals and experimental protocols

All animal experiments in this study were approved by the Ethics Committee of Nanjing Medical University (IACUC-2011003) and conducted according to the European Convention for the Protection of Vertebrate Animals used for Experimental and other Scientific Purposes. A total of 30 five-week-old Sprague-Dawley rats were provided by Nanjing Medical University Laboratory Animal Center. After a one-week adaptation period, 24 rats were fed a high-fat diet (HFD) for 4 weeks and then given a single intraperitoneal (i.p.) injection of streptozotocin (STZ, 35 mg/kg) to induce type 2 diabetes (T2D), while six rats received standard commercial rat chow and an i.p. injection of an equal volume of citrate buffer served as the control group. After successful induction of T2D, the 24 diabetic rats were randomly divided into two groups by a random number method: the RDN group (n = 12), which received real RDN surgery and HFD for another 8 weeks; the DCM group (n = 12), which received sham RDN surgery and HFD for another 8 weeks; and the six rats in the control group, which received sham RDN surgery and standard commercial rat chow for 8 weeks. Sham surgery or RDN treatment was performed bilaterally 1 week after the STZ injection. All animals were housed in a room with controlled temperature and humidity, a 12-h light/dark cycle, and ad libitum access to drinking water. All data from this research were collected under blinded conditions.

To verify that the therapeutic effect of RDN on DCM is mediated by the regulation of renal SGLT2 expression, a separate experiment was carried out on an additional 40 Sprague-Dawley rats. After successful induction of T2D, 40 diabetic rats were randomly divided into four groups: the DCM group ($n = 10$), which received sham RDN surgery and normal saline; the RDN group ($n = 10$), which received real RDN surgery and normal saline; the SGLT2 inhibitor (SGLT2i) group ($n = 10$), which received sham RDN surgery and SGLT2i treatment; and the RDN + SGLT2i group ($n = 10$), which received real RDN surgery and SGLT2i treatment. One week after the STZ injection, all rats were fed a HFD for another 8 weeks. Sham surgery or real RDN surgery was performed bilaterally 1 week after the STZ injection. Empagliflozin (Boehringer Ingelheim Pharma GmbH & Co KG, Biberach, Germany) or normal saline was administered intragastrically at a dosage of 20 mg/kg/day for 8 weeks beginning in the fifth week[23].

Diabetic cardiomyopathy model

DCM was established using a T2D model[24]. To induce T2D, rats were fed a HFD (D12492, fat energy ratio = 60 kcal%; Research Diets, New Brunswick, New Jersey, USA) for four weeks. On the 28th day, rats were fasted overnight and then given a single i.p. injection of low-dose STZ (35 mg/kg; Sigma-Aldrich, St. Louis, MO, USA), which was dissolved in citrate buffer (0.1 mol/L, pH 4.5, 4 °C). One week following the STZ injection, blood samples were collected from the tail vein to measure the blood glucose level. Rats with fasting blood glucose (FBG) ≥ 11.1 mmol/L or random blood glucose ≥16.7 mmol/L were considered diabetic and fed a HFD for another 8 weeks. Rats in the control group received only standard commercial rat chow for 13 weeks, and they were given a single i.p. injection of an equivalent volume of citrate buffer in the 4th week.

Renal denervation

One week after STZ injection, rats in all groups were subjected to RDN or sham RDN surgery. The detailed surgical procedures for RDN were as follows. First, the rats were anesthetized with 2% sodium pentobarbital by i.p. injection (50 mg/kg). Next, the skin was cut ~3 cm below the costal-spinal angle to locate the kidneys and perirenal adipose tissue. Once the renal vessels were fully exposed, all visible nerves were severed by a glass dissecting needle. Next, 20% phenol dissolved in alcohol was painted on bilateral renal vessels to destroy the remaining nerves. Rats in the DCM group and the control group were subjected to the same procedures but without destruction of the bilateral renal nerves. The rats were given carprofen (5 mg/kg, subcutaneous injection) 10 min before anesthesia to relieve pain and penicillin (400,000 U/day, intramuscular injection) for 3 days to prevent infection[25, 26].

Metabolic cage study

At week 12, a metabolic cage study was performed to collect urine samples. In detail, each rat was placed into an individual metabolic cage. All rats maintained their high-fat chow or standard commercial rat chow and had free access to water. After a one-week adaptation period (with no significant changes in body weight), the 24-h fluid intake and urine volume of rats were recorded, and 24-hour urine samples were collected for urine glucose assessment.

Echocardiography and blood pressure measurement

At week 13, echocardiography was performed to evaluate cardiac systolic and diastolic function using a Vevo2100 (VisualSonics, Toronto, Canada) system. Cardiac systolic function was evaluated by left ventricular ejection fraction (EF) and fractional shortening (FS), while cardiac diastolic function was assessed by the E/A ratio (early diastolic inflow E-wave, late diastolic inflow A-wave, E/A = ratios of E to A waves) as well as the E/E′ ratio (early diastolic inflow E-wave, early diastolic annular e′-wave, E/E′ = ratios of E to E′ waves). A non-invasive computerized tail-cuff system (Kent Scientific, Torrington, CT, USA) was used to measure blood pressure. The systolic blood pressure (SBP) and diastolic blood pressure (DBP) were obtained in the tail artery of conscious rats.

Small-animal PET imaging

At week 13, a fluorodeoxyglucose (^{18}F)-positron emission tomography/computed tomography (^{18}F-FDG PET/CT) imaging protocol was performed to evaluate cardiac glucose metabolism. All rats were fasted overnight before examination. Anesthesia was induced and maintained throughout the scanning procedure by isoflurane inhalation. PET/CT measurements were performed on a 3-dimensional small-animal MicroPET system (Siemens, Berlin, Germany), and ^{18}F-FDG was synthesized in-house as an imaging agent (Nanjing First Hospital, Nanjing, China). All rats were injected with ~400 μCi ^{18}F-FDG via the tail vein and allowed to move freely for 45 min. Then, a 10-min PET scan was obtained under isoflurane anesthesia. The standardized uptake value (SUV) was calculated to characterize the myocardial ^{18}F-FDG uptake level.

Biochemical parameter analysis

At the end of the experiment, the control, DCM and RDN groups included six, nine and ten rats that survived all procedures, respectively. Before sacrifice, all rats were fasted overnight, and blood samples were collected from the inferior vena cava under anesthesia. Levels of serum total cholesterol (TC), high-density lipoprotein cholesterol (HDL-C), low-density lipoprotein cholesterol (LDL-C), triglyceride (TG) and FBG were detected using a Roche Cobas 8000 modular analyzer system (Roche, Rotkreuz, Switzerland). In addition, urinary glucose concentration was also measured by the same method.

Histopathology
All rats were sacrificed by an overdose of pentobarbital sodium (200 mg/kg), and then the heart, kidneys, and renal vessels were collected after perfusion with normal saline. Each harvested heart was weighed and used to calculate the ratio of heart weight to body weight (HW/BW). Hematoxylin-eosin (HE) staining was used to evaluate the cardiac pathological changes. Masson's trichrome staining was performed to assess myocardial fibrosis, and the collagen volume fraction (CVF) was quantified to determine the extent of fibrosis. Heart sections were stained with periodic acid-Schiff (PAS) reagent to evaluate glycogen content, while myocardial frozen sections were stained with oil red-O to detect lipid accumulation. All images were processed using Image-Pro Plus 6.0 software (National Institutes of Health, NIH, Bethesda, Maryland, USA).

Immunohistochemistry
To verify the efficacy of RDN, renal vessels and renal cortex were stained with an anti-tyrosine hydroxylase (TH) antibody (Abcam, Cambridge, UK) to identify renal sympathetic nerves. Heart sections were stained with anti-glucose transporter 4 (GLUT4) antibody (Abcam, Cambridge, UK) and anti-fatty acid transporter (FAT/CD36) antibody (Abcam, Cambridge, UK) to evaluate the myocardial glucose uptake and fatty acid uptake levels. In addition, immunohistochemical (IHC) staining with an anti-AGE antibody (Bioss, Beijing, China) was performed to quantify the generation of AGEs in cardiac tissues. Five fields were randomly selected for analysis, and the integrated optical density (IOD) per field was measured by Image-Pro Plus 6.0 software (NIH, Bethesda, Maryland, USA).

Immunofluorescence
Immunofluorescence (IF) staining with an anti-SGLT2 antibody (Proteintech, Rosemont, Illinois, USA) was performed to detect the distribution of SGLT2 in the kidney. Wheat germ agglutinin (WGA) staining was performed to quantify the diameters of cardiomyocytes in the heart tissues. Five fields were randomly selected for analysis, and the myocyte size was calculated by ImageJ software (NIH, Bethesda, Maryland, USA).

Measurement of myocardial mitochondrial membrane potential
Mitochondria were isolated from fresh cardiac tissues according to the instructions of the Mitochondria Isolation Kit (Beyotime Biotechnology, Shanghai, China). The mitochondrial membrane potential (MMP) was detected using a JC-1 detection kit (Beyotime Biotechnology, Shanghai, China). The level of MMP was reflected by the ratio of red and green fluorescence intensity[27].

Electron microscopy
Transmission electron microscopy (JEM 1200, Tokyo, Japan) was used to observe the morphological changes of mitochondria in the heart tissues. In brief, ~1 mm^3 of tissue was quickly removed from the left ventricular myocardium. These specimens were immediately immersed in 2.5% glutaraldehyde buffer for 24 h and then fixed with 1% buffered osmium tetroxide for postfixation. After dehydration and embedding, these specimens were cut into 70 nm slices and observed using electron microscopy after double staining with lead citrate and uranyl acetate.

Western blotting
Western blotting (WB) was used to semiquantitatively analyze the expression levels of related proteins. Total proteins, sarcolemmal proteins and mitochondrial proteins in the tissue homogenates were extracted according to the manufacturer's instructions (Beyotime Biotechnology, Shanghai, China). The bicinchoninic (BCA) method or Bradford method was used to detect the protein concentrations in all groups. After electrophoresis, transfer, and blocking, these samples were probed with specific primary antibodies, including anti-SGLT2 (Abcam, Cambridge, UK), anti-GLUT4 (Abcam, Cambridge, UK), anti-FAT/CD36 (Abcam, Cambridge, UK), anti-PDH (pyruvate dehydrogenase, Cell Signaling Technology, Boston, Massachusetts, USA), anti-CPT1 (carnitine palmitoyltransferase-1, Abcam, Cambridge, UK), anti-BDH1 (3-hydroxybutyrate dehydrogenase 1, Cell Signaling Technology, Boston, Massachusetts, USA), anti-SCOT (succinyl CoA:3-oxoacid CoA transferase, Cell Signaling Technology, Boston, Massachusetts, USA) and anti-O-GlcNAc (Bioss, Beijing, China). Then, the membranes were incubated with the appropriate secondary antibodies. Protein bands were visualized via enhanced chemiluminescence and analyzed with ImageJ software (NIH, Bethesda, Maryland, USA).

Enzyme-linked immunosorbent assay
The activities of PDH, CPT1, BDH1 and SCOT in the cardiac tissues were detected with a commercial ELISA kit according to the manufacturer's protocol (mlbio, Shanghai, China). The concentrations of cardiac AGEs, ceramide, FFAs and serum fasting insulin were measured with a commercial ELISA kit according to the manufacturer's instructions (mlbio, Shanghai, China). The level of renal norepinephrine (NE) was measured by using a commercial ELISA kit (Cusabio, Wuhan, China). The levels of mitochondrial ATP and the activities of complexes I-V in the myocardium were measured according to instructions provided by commercial ELISA kits (Nanjing Jiancheng Bioengineering Institute, Nanjing, China).

Statistical analysis
All data in this study were analyzed and processed using SPSS 16.0 software (SPSS, USA). For two-group comparisons, data were analyzed with two-tailed unpaired t-tests. For multiple-group comparisons, data were processed using one-way ANOVA followed by the Newman-Keuls test. Fisher's exact test was used for qualitative data analysis. Quantitative data are presented as the mean ± standard deviation (SD). $P < 0.05$ was considered indicative of statistical significance.

RESULTS
RDN removed renal sympathetic nerves and attenuated sympathetic activity
Tyrosine hydroxylase is a key enzyme involved in catecholamine biosynthesis[28]. We first evaluated the efficacy of RDN in removing renal sympathetic nerves by TH staining of the renal vessels and renal cortex. As shown in Fig. 1A, RDN effectively reduced the TH intensity around the renal artery and the TH density in the renal cortex compared with sham RDN. Kidney norepinephrine level is another important biomarker for assessing renal sympathetic outflow[29]. There was a significant decrease in renal NE in the RDN group compared with that in the control group and the DCM group. Together, these results verified the high efficacy of RDN in ablating renal nerves and inhibiting sympathetic activity.

RDN promoted urinary glucose excretion by downregulating the expression of renal SGLT2
SGLT2, a sodium-glucose cotransporter located in the proximal tubule of the kidney, is responsible for the majority of glucose reabsorption in the kidney[30]. As shown in Fig. 1B, representative photomicrographs demonstrated that the expression of renal SGLT2 was significantly increased in the DCM group but markedly decreased in the RDN group. Consistent with this finding, WB results also showed that RDN effectively attenuated the overexpression of renal SGLT2 induced by T2D.

Considering the important role of SGLT2 in urinary glucose reabsorption, we also collected urine samples through a metabolic cage study. Compared with the rats in the control group, the 24-hour urine volume and urinary glucose concentration of diabetic rats were significantly increased, and RDN further augmented the urinary glucose concentration and increased the 24-hour urine volume, thus promoting urinary glucose excretion (UGE). Accordingly, these findings demonstrated that RDN could facilitate UGE by regulating the expression of SGLT2 in the kidney.

RDN regulated systemic metabolic disorders
Urinary glucose reabsorption is closely related to blood glucose homeostasis. Therefore, we further assessed the effect of RDN on systemic glucose metabolism. The blood biochemical parameters indicated that diabetic rats had hyperglycemia and hyperinsulinemia. In addition, lipid metabolism-related indicators such as triglycerides and total cholesterol were also significantly increased in the DCM group. RDN effectively reduced fasting blood glucose and fasting insulin. Furthermore, RDN decreased the levels of

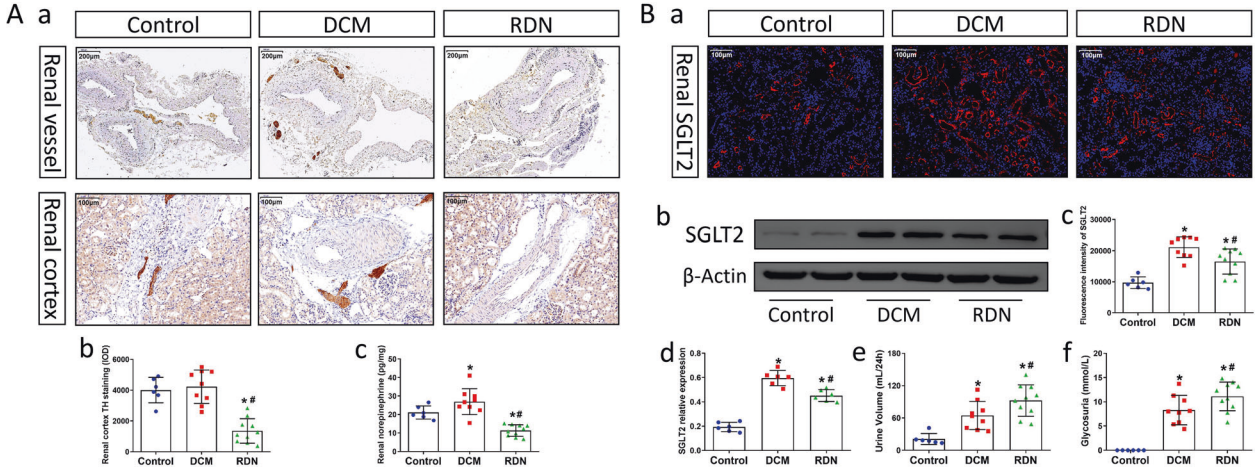

Fig. 1 RDN effectively promoted urinary glucose excretion in DCM rats. A RDN removed renal sympathetic nerves and attenuated sympathetic outflow. **a** Representative images of TH immunohistochemical staining in the renal vessels (magnification, 100×) and renal cortex (magnification, ×200). **b** Quantitative analysis of TH-positive areas in the renal cortex. **c** ELISA quantification of renal norepinephrine levels. **B** RDN facilitated UGE by regulating renal SGLT2 expression. **a** Representative images of SGLT2 immunofluorescence staining in the kidney (magnification, ×200). **b** WB analysis of protein levels of SGLT2 in the kidney. **c** Quantitative analysis of SGLT2 fluorescence intensity in the kidney. **d** The relative levels of SGLT2 calculated from the WB. **e** The 24-h urine volume of rats from three groups collected in the metabolic cage study. **f** Urinary glucose concentration of rats from three groups. ($P < 0.05$; $n = 6$, 9, and 10 in the control, DCM, and RDN groups, respectively; five sections were randomly selected per sample.) *$P < 0.05$ vs. the control group; #$P < 0.05$ vs. the DCM group. RDN renal denervation, DCM diabetic cardiomyopathy, TH tyrosine hydroxylase, UGE urinary glucose excretion, SGLT2 sodium-glucose cotransporter 2.

serum TC, LDL-C and triglyceride (all data are presented in Table 1). In summary, these results suggested that RDN had a beneficial effect on systemic metabolic abnormalities.

RDN improved diastolic function and cardiac remodeling in diabetic cardiomyopathy

DCM is a serious T2D-related cardiovascular complication and is closely related to systemic metabolic disorders[31]. As shown in Fig. 2A, echocardiography demonstrated that rats in the DCM group exhibited an enlarged left atrial diameter (LAD) and thickened left ventricular wall. A reversed E/A ratio and an increased E/E′ ratio were also observed in the DCM group, suggesting that diabetic rats developed diastolic dysfunction. In addition, we evaluated the cardiac pathological changes in the hearts of diabetic rats. As shown in Fig. 2B, the HW/BW ratio was significantly elevated in the DCM group. Consistent with this finding, myocyte size calculated from cardiac WGA staining was also significantly increased in the DCM group, suggesting that myocardial hypertrophy occurred in the diabetic rats. Furthermore, cardiac HE staining revealed that hypertrophic myocardial cells were arranged in a disorderly manner with inflammatory cell infiltration. Cardiac Masson staining showed that diabetic rats generated obvious perivascular and interstitial fibrosis. All of the above results suggested that diabetic rats developed cardiac dysfunction and pathological remodeling. However, compared with those in the DCM group, rats in the RDN group showed decreased LAD and E/E′ ratios as well as normalized E/A ratios. In addition, RDN also reduced the myocyte size and mitigated interstitial fibrosis. These results all confirmed that RDN could effectively improve cardiac dysfunction and pathological remodeling caused by DCM.

RDN ameliorated myocardial glucose metabolism in diabetic cardiomyopathy

Cardiac metabolic abnormalities are an important component of the progression of DCM. We next evaluated the effects of RDN on substrate metabolism. We first assessed the role of RDN in myocardial glucose metabolism.

First, ^{18}F-FDG PET/CT in vivo demonstrated that rats in the DCM group exhibited significantly lower cardiac glucose uptake than rats in the control group, while compared with rats in the DCM group, rats in the RDN group showed higher cardiac glucose uptake, as evidenced by the SUV level (Fig. 3Aa, c). Similarly, the results from IHC and WB led to the same conclusion. GLUT4, a glucose transporter mainly stored in intracellular compartments, can be translocated to the sarcolemma under various stimuli, thus playing an important role in myocardial glucose uptake[32]. As shown in Fig. 3A, the majority of GLUT4 in the control group and the RDN group gathered near the sarcolemma, while GLUT4 in the DCM group was mainly distributed in the cytosolic fraction. In addition, WB results showed that the expression of sarcolemmal GLUT4 was significantly reduced in the DCM group, while RDN preserved the expression of GLUT4 in the sarcolemma. All of the above results indicated that RDN could restore myocardial glucose uptake.

Second, we assessed myocardial glucose oxidation. PDH is an important rate-limiting enzyme for glucose aerobic oxidation[33]. Compared with those in the control group, both the protein level and enzyme activity of PDH decreased significantly in the DCM group, indicating that DCM impaired the utilization of glucose in the myocardium. In contrast, RDN increased the expression and activity of PDH in cardiac tissues, thus partially restoring myocardial glucose utilization.

Third, we detected various glycotoxic products in the myocardium. As shown in Fig. 3C, DCM caused the accumulation of glycogen and AGEs in cardiac tissues. Furthermore, quantitative detection of AGEs in myocardial homogenates also demonstrated the same results. In addition, hearts from diabetic rats in the DCM group had a higher O-GlcNAcylation of various proteins. However, RDN markedly decreased the deposition of glycogen and AGEs in the myocardium, as well as the level of O-GlcNAcylation. These results suggested that RDN could alleviate cardiac glucotoxicity. In summary, RDN promoted myocardial glucose uptake and utilization but attenuated the detrimental effects of glucotoxicity on the myocardium.

RDN regulated myocardial fatty acid metabolism in diabetic cardiomyopathy

The relationship between glucose utilization and FFA utilization is reciprocal and governed by the Randle cycle in the heart[31]. Since

RDN acted on myocardial glucose metabolism, we next evaluated the effects of RDN on myocardial fatty acid metabolism.

First, we evaluated myocardial FFA uptake in the hearts of all groups. FAT/CD36 is one of the main transporters involved in FA uptake. FAT/CD36 can translocate from intracellular vesicles to the plasma membrane to increase myocardial FA absorption[34]. As shown in Fig. 4A, compared with that in the control group, CD36 in the DCM group mainly gathered near the sarcolemma. RDN induced the translocation of CD36 back to the cytoplasm, thereby reducing the uptake of FAs. Similarly, the expression of sarcolemmal CD36 increased in the hearts of the DCM group but decreased in the hearts of the RDN group. These results suggested that RDN could reduce the excessive uptake of FAs in DCM.

Second, we assessed the level of FA oxidation in the myocardium. CPT1 is a rate-limiting enzyme for mitochondrial uptake of FAs and plays a crucial role in FA metabolism[35]. As shown in Fig. 4B, the expression and activity of CPT1 in the myocardial homogenates were significantly increased in the DCM group, suggesting that hearts of diabetic rats were more dependent on FA oxidation for ATP production. No change was observed in CPT1 activity or expression between the RDN group and the DCM group.

Third, we evaluated lipotoxicity in the hearts of all groups. As shown in Fig. 4C, oil red O staining showed that myocardial lipid accumulation was significantly increased in the DCM group. In addition, the levels of toxic metabolites, including ceramide and triglycerides, were also elevated in the DCM group. In contrast, RDN alleviated myocardial lipid deposition and reduced ceramide and triglyceride levels. In conclusion, we found that RDN could reduce the uptake of FAs, maintain the utilization of FAs and thus attenuate the accumulation of lipotoxic products.

Table 1. RDN improved cardiac hypertrophy and systemic metabolic disorders.

	Control	DCM	RDN
Body weight (g)	436.0 ± 27.36	445.1 ± 39.11	395.7 ± 56.80
Heart weight (g)	1.11 ± 0.13	1.52 ± 0.10*	1.22 ± 0.17#
HW/BW (mg/g)	2.55 ± 0.26	3.44 ± 0.30*	3.11 ± 0.52*
FBG (mmol/L)	5.57 ± 0.74	16.67 ± 2.07*	13.87 ± 2.51*#
FINS (mIU/L)	14.86 ± 4.09	44.60 ± 7.66*	31.61 ± 9.52*#
LDL-C (mmol/L)	0.30 ± 0.03	0.43 ± 0.08*	0.34 ± 0.08#
HDL-C (mmol/L)	0.71 ± 0.05	0.70 ± 0.11	0.74 ± 0.13
TC (mmol/L)	1.25 ± 0.12	2.42 ± 0.23*	1.87 ± 0.38*#
TG (mmol/L)	0.46 ± 0.07	1.27 ± 0.21*	0.69 ± 0.27*#
FFA (mmol/L)	0.69 ± 0.03	0.96 ± 0.07*	0.98 ± 0.09*
SBP (mmHg)	114.72 ± 14.16	124.23 ± 20.30	117.53 ± 12.94
DBP (mmHg)	83.25 ± 9.05	92.70 ± 23.67	86.69 ± 8.63

Data are presented as the mean ± SD. *$P < 0.05$ vs. the control group; #$P < 0.05$ vs. the DCM group.
RDN renal denervation, *FBG* fasting blood glucose, *FINS* fasting insulin, *LDL-C* low-density lipoprotein cholesterol, *HDL-C* high-density lipoprotein cholesterol, *TC* total cholesterol, *TG* triglyceride, *FFA* free fatty acids, *SBP* systolic blood pressure, *DBP* diastolic blood pressure.

RDN promoted the use of ketone bodies as a supplemental fuel in diabetic cardiomyopathy

As an alternative energy source, KBs are characterized by high efficiency and low oxygen consumption. The role of KBs in DCM is

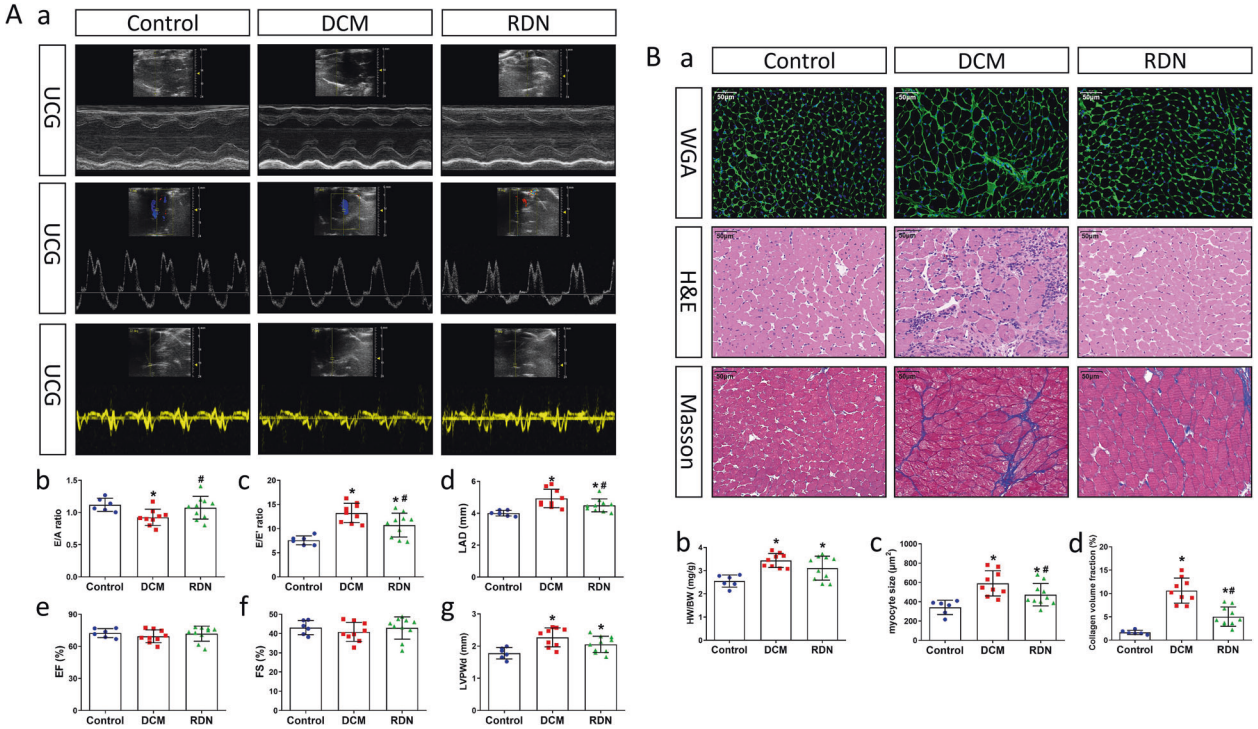

Fig. 2 RDN ameliorated DCM-induced cardiac dysfunction and pathological remodeling. **A** RDN improved cardiac diastolic dysfunction. **a** Representative tracings of echocardiography. **b** E/A ratio. **c** E/E′ ratio. **d** LAD. **e** EF. **f** FS. **g** LVPWd. **B** RDN prevented cardiac pathological remodeling. **a** Representative images of WGA staining (magnification, ×400), HE staining (magnification, ×400) and Masson staining (magnification, ×400) in the hearts. **b** HW/BW ratio. **c** Quantitative analysis of myocyte size calculated from WGA staining. **d** Quantitative analysis of CVF calculated from Masson staining. ($P < 0.05$; $n = 6$, 9, and 10 in the control, DCM, and RDN groups, respectively; five sections were randomly selected per sample.) *$P < 0.05$ vs. the control group; #$P < 0.05$ vs. the DCM group. LAD left atrial diameter, EF ejection fraction, FS fractional shortening, LVPWd left ventricular posterior wall diastolic thickness, WGA wheat germ agglutinin, CVF collagen volume fraction.

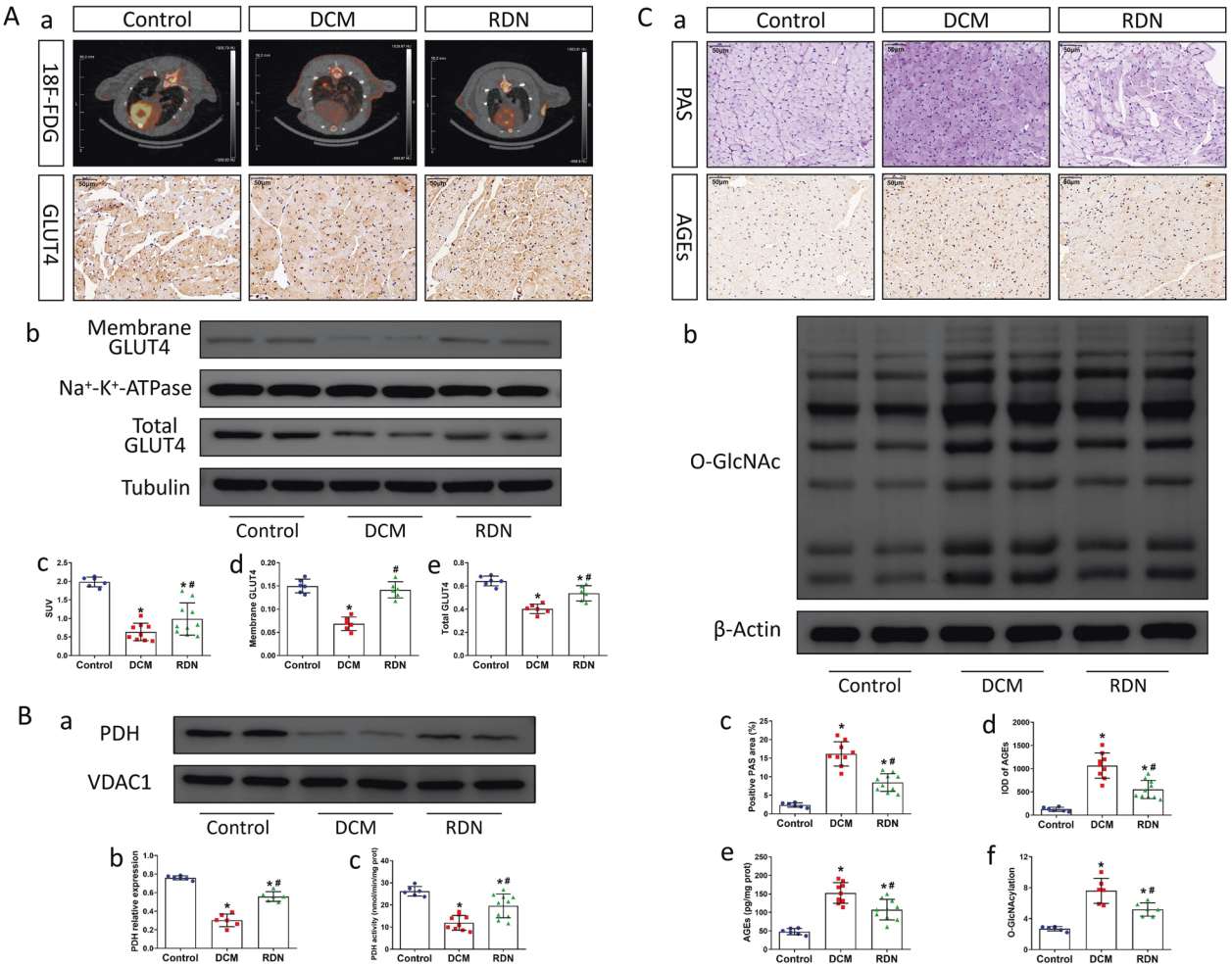

Fig. 3 RDN improved myocardial glucose metabolism abnormalities. A RDN facilitated myocardial glucose uptake. **a** Representative images of ^{18}F-FDG PET/CT and GLUT4 immunohistochemical staining in the myocardium (magnification, ×400) of rats from the three groups. **b** WB analysis of the protein levels of sarcolemmal GLUT4 and total GLUT4 in the heart. **c** Quantitative analysis of SUV calculated from ^{18}F-FDG PET/CT images. **d**–**e** The relative levels of sarcolemmal GLUT4 and total GLUT4 calculated from WB. **B** RDN enhanced myocardial glucose utilization. **a** WB analysis of protein levels of PDH in the hearts. **b** The relative levels of PDH calculated from WB. **c** ELISA quantification of myocardial PDH activity. **C** RDN alleviated myocardial glucotoxicity. a Representative images of PAS staining (magnification, ×400) and AGEs immunohistochemical staining (magnification, ×400) in the hearts of rats from the three groups. **b** WB analysis of protein levels of O-GlcNAcylation in the hearts. **c** Quantitative analysis of PAS-positive areas in the hearts. **d** Quantitative analysis of AGEs-positive regions in the heart. **e** ELISA analysis of myocardial AGEs levels. **f** The relative levels of O-GlcNAcylation calculated from WB. ($P < 0.05$; $n = 6$, 9, and 10 in the control, DCM, and RDN groups, respectively; five sections were randomly selected per sample.) *$P < 0.05$ vs. the control group; #$P < 0.05$ vs. the DCM group. GLUT4 glucose transporter 4, SUV standardized uptake value, AGEs advanced glycation end products, PDH pyruvate dehydrogenase.

still unknown. Therefore, we further evaluated the effect of RDN on myocardial KB metabolism. As shown in Fig. 4D, BDH1 and SCOT are important rate-limiting enzymes for KB utilization in the mitochondria. The protein expression and enzyme activity of BDH1 in the myocardium were significantly decreased under diabetic conditions. In addition, the enzyme activity of SCOT was also reduced, although the protein expression showed no change. RDN increased the expression and activity of BDH1, as well as the enzyme activity of SCOT, suggesting that RDN could improve DCM-induced inhibition of ketone metabolism.

RDN ameliorated mitochondrial dysfunction in diabetic cardiomyopathy

In light of the mitochondrial damage caused by glucotoxicity and lipotoxicity, we further evaluated the effect of RDN on mitochondrial function in the DCM model. As shown in Fig. 5, electron microscopy images showed that the mitochondria of the myocardium were conspicuously damaged under diabetic conditions, as observed by the large, swollen mitochondria with an extensive loss of cristae. RDN ameliorated these mitochondrial morphological abnormalities caused by DCM. In addition to mitochondrial morphology, we also evaluated the enzyme activity of the mitochondrial electron respiratory chain. The activities of complexes I, II, III, IV and V were significantly decreased in the DCM group. RDN partially restored the activity of complexes I, III and IV. As a result, the level of mitochondrial ATP was decreased in the DCM group but increased in the RDN group. In addition, MMP is an important indicator for assessing mitochondrial function. The results shown in Fig. 5G demonstrated that the MMP in the DCM group declined to different degrees, but RDN treatment significantly improved the MMP. In summary, RDN could improve mitochondrial morphological and functional abnormalities caused by DCM, thereby promoting ATP production.

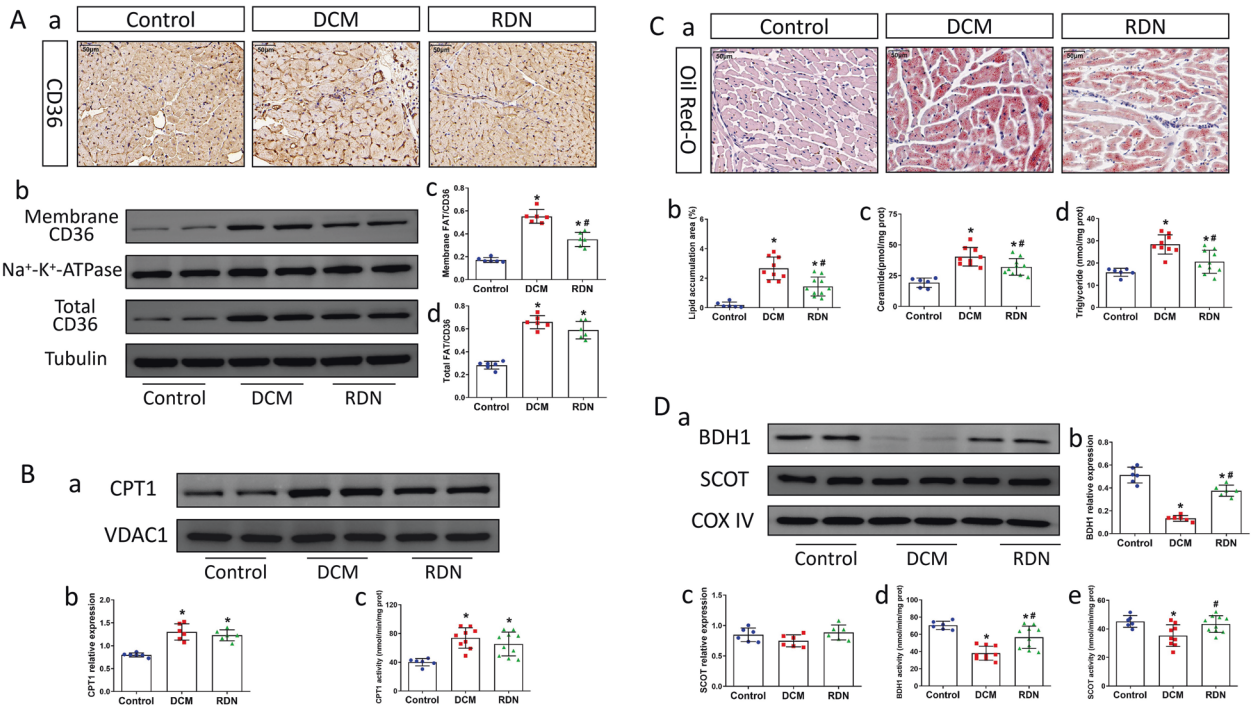

Fig. 4 RDN regulated myocardial lipid metabolism and promoted the utilization of ketone bodies. A RDN reduced myocardial fatty acid uptake. **a** Representative images of CD36 immunohistochemical staining in the myocardium (magnification, ×400) of rats from the three groups. **b** WB analysis of the protein levels of sarcolemmal CD36 and total CD36 in the hearts. **c**, **d** The relative levels of sarcolemmal CD36 and total CD36 calculated from WB. **B** RDN maintained myocardial FFA oxidation. **a** WB analysis of protein levels of CPT1 in the hearts. **b** The relative levels of CPT1 calculated from WB. **c** ELISA quantification of myocardial CPT1 activity. **C** RDN alleviated myocardial lipotoxicity. **a** Representative images of oil red O staining (magnification, ×400) in the hearts. **b** Quantitative analysis of lipid accumulation in the heart. **c** ELISA quantification of myocardial ceramide levels. **d** ELISA quantification of myocardial triglyceride levels. **D** RDN promoted the use of KBs as a supplemental fuel. **a** WB analysis of the protein levels of BDH1 and SCOT in the heart. **b**, **c** The relative levels of BDH1 and SCOT calculated from WB. **d**, **e** ELISA quantification of myocardial BDH1 and SCOT activity. ($P < 0.05$; $n = 6$, 9, and 10 in the control, DCM, and RDN groups, respectively; five sections were randomly selected per sample.) *$P < 0.05$ vs. the control group; #$P < 0.05$ vs. the DCM group. CD36 fatty acid transporter, FFA free fatty acids, CPT1 carnitine palmitoyltransferase-1, BDH1 3-hydroxybutyrate dehydrogenase 1, SCOT succinyl CoA:3-oxoacid CoA transferase.

The protective effects of RDN against diabetic cardiomyopathy are mediated by regulation of renal SGLT2 expression

To further confirm that the therapeutic effect of RDN on DCM is mediated by regulating renal SGLT2 expression, we conducted a separate experiment to elucidate the mechanism by adding an SGLT2 inhibitor. As shown in Fig. 6, both RDN and SGLT2i decreased cardiac AGEs levels and O-GlcNAcylation, suggesting that both treatments could alleviate the glycotoxicity caused by DCM. However, the combination of RDN and SGLT2i did not further ameliorate glycotoxicity. In addition, both RDN and SGLT2i improved DCM-induced lipotoxicity, but the combination of RDN and SGLT2i had no additive therapeutic effect. Finally, we also evaluated cardiac mitochondrial damages in all groups and observed that the combination of RDN and SGLT2i did not further improve mitochondrial dysfunction compared with the RDN group or the SGLT2i group alone. In summary, these results collectively verified that the therapeutic effect of RDN on DCM is mediated by the regulation of renal SGLT2 expression.

Comparison between RDN and SGLT2i on the effect of DCM

As shown in Fig. 6, RDN and SGLT2i showed similar effects in improving cardiac metabolic disorders and mitochondrial damage. On this basis, we further compared their effects on cardiac function and pathological changes in the DCM model. Echocardiography results showed that both RDN and SGLT2i improved diabetes-induced diastolic dysfunction, and no significant difference was observed between the RDN group and the SGLT2i group (Fig. 7A). In addition, the histopathology results also suggested that RDN was not inferior to SGLT2i in delaying cardiac pathological remodeling, as evidenced by cardiac WGA staining, HE staining and Masson staining (Fig. 7B). In summary, these results collectively verified that the therapeutic effect of RDN on DCM is not inferior to that of SGLT2i.

DISCUSSION

In this study, we established a DCM model to evaluate the effect of RDN on cardiac energy metabolism and mitochondrial function. The major findings were as follows: (1) RDN effectively downregulated the expression of renal SGLT2, promoted UGE and decreased blood glucose concentration; (2) RDN improved cardiac diastolic dysfunction and prevented the progression of cardiac remodeling; (3) RDN attenuated cardiac glucose and lipid metabolism disorders, thus reducing cardiac glucotoxicity and lipotoxicity; and (4) RDN protected mitochondria from damage induced by glucotoxicity and lipotoxicity, ameliorated mitochondrial dysfunction and increased mitochondrial ATP production.

RDN and SGLT2

Recently, crosstalk between SGLT2 and the autonomic nervous system (ANS) has attracted widespread attention. Matthews et al. found that dapagliflozin markedly decreased HFD-induced elevations in TH and NE levels in the heart and kidney[36]. Similarly, empagliflozin was shown to normalize heart rate baroreflexes and renal sympathetic reflexes in a diabetic rabbit model[37]. Several clinical studies also confirmed the important role of SGLT2i in regulating the ANS. Jordan et al. found that empagliflozin

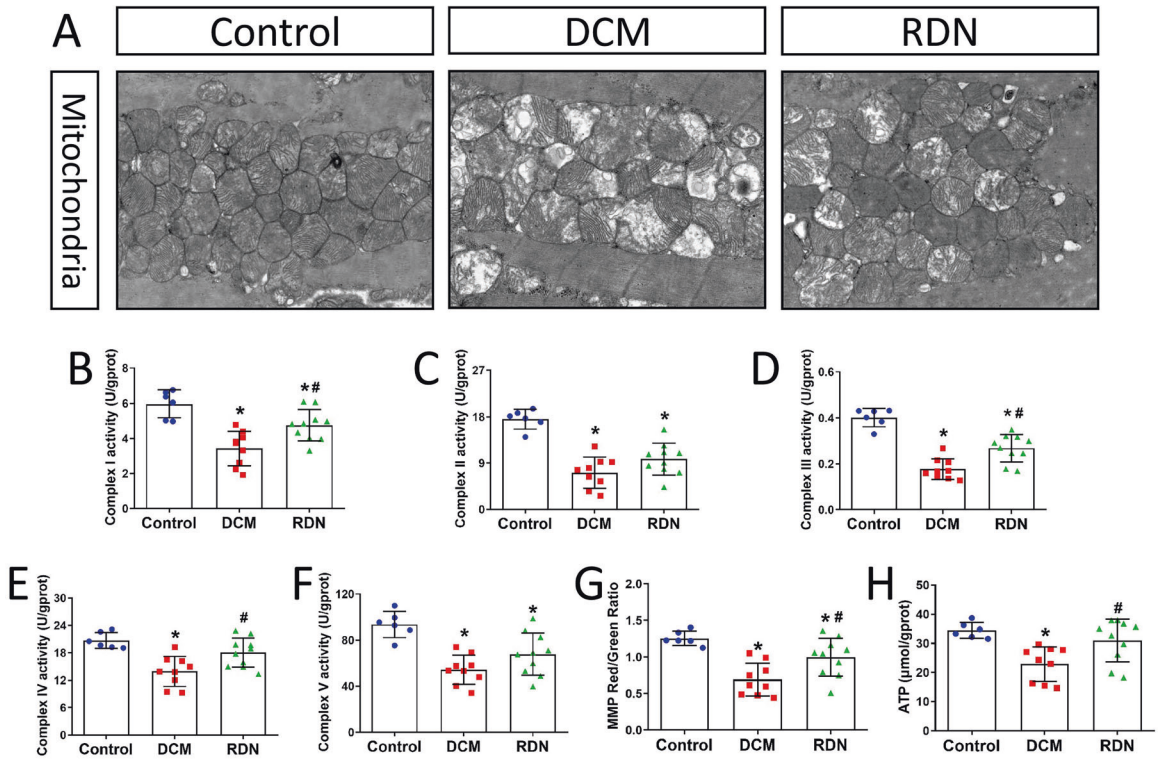

Fig. 5 RDN ameliorated mitochondrial dysfunction in DCM rats. A Representative images of mitochondria (magnification, ×7000) of rats from the three groups. **B**–**F** The activity of respiratory chain enzyme complexes I, II, III, IV, and V measured by ELISA. **G** The analysis of mitochondrial membrane potential. **H** ELISA quantification of myocardial ATP levels. ($P < 0.05$; $n = 6$, 9, and 10 in the control, DCM, and RDN groups, respectively.) *$P < 0.05$ vs. the control group; #$P < 0.05$ vs. the DCM group.

eliminated reflex-mediated sympathetic overactivation in patients with T2D[38]. In summary, the regulatory effect of SGLT2i on the ANS has been widely recognized, especially in diseases with sympathetic overactivity, such as prediabetes, obesity, T2D and metabolic syndrome. However, the role of the ANS in SGLT2 needs to be further elucidated. Matthews *et al*. found that norepinephrine could significantly elevate the expression of SGLT2 in human renal proximal tubule cells and facilitate the translocation of SGLT2 to the cell surface[36]. In our study, we evaluated the sympathetic inhibitory effect of RDN on renal SGLT2 expression. IF staining showed that RDN significantly reduced the distribution of SGLT2 in the kidney. WB analysis confirmed that RDN decreased the protein levels of SGLT2 in renal homogenates. Furthermore, the increased urinary glucose concentration and 24-hour urine volume further illustrated the effectiveness of RDN on SGLT2 inhibition.

RDN and energy metabolism

Abnormal myocardial metabolism is an important factor leading to the progression of DCM, especially disturbed glucose metabolism[4]. Disorders of glucose metabolism present as reduced myocardial glucose uptake, reduced pyruvate oxidation, and the accumulation of glycolytic intermediates as well as O-GlcNAcylation[8]. Numerous studies have confirmed the beneficial effects of restoring glucose metabolism in DCM. Verma *et al*. found that an increase in the rate of glucose oxidation could significantly augment cardiac ATP production and prevent cardiac failure in diabetic mice[39]. Furthermore, Ramírez et al. demonstrated that the protective effect of the GLP-1 enhancer on cardiac function is mediated by shifting from FA to glucose utilization in a T2D rat model[40]. In the present study, we observed that RDN increased the protein levels of sarcolemmal GLUT4 and promoted the translocation of GLUT4 to the cell surface, thus partially restoring myocardial glucose uptake. Moreover, RDN facilitated the utilization of pyruvate, as reflected by enhanced PDH expression and activity. In addition, RDN attenuated the accumulation of glycolytic intermediates and alleviated glucotoxicity. All these results indicated that RDN could correct glucose metabolism disturbances caused by DCM.

Lipid metabolism disorders are another hallmark of energy metabolism in DCM and are characterized by increased FA uptake, elevated FA β-oxidation, and the deposition of toxic lipid metabolites[41]. These metabolic disturbances can reduce cardiac efficiency by increasing oxygen consumption, ultimately causing cardiac dysfunction. Therefore, the normalization of myocardial lipid metabolism is an important therapeutic strategy. In the present study, we observed that RDN decreased the expression of sarcolemmal CD36 and promoted the translocation of CD36 back to the cytoplasm, thus attenuating myocardial FFA uptake. In addition, RDN significantly reduced lipid metabolite deposition, thus ameliorating the cellular damage caused by lipotoxicity. We speculated that this phenomenon may be due to RDN reducing the uptake of FAs but maintaining the rate of FA oxidation. Ketone bodies, with a relatively high phosphate/oxygen ratio, are regarded as a thrifty substrate[42]. The beneficial effects of KBs on heart failure have been extensively studied[43], but their role in DCM is still controversial. Our study demonstrated that RDN could promote the utilization of myocardial ketone bodies. In summary, we discovered for the first time that RDN can regulate SGLT2 and glucose homeostasis, which regulates cardiac metabolic abnormalities and provides a potential strategy for the treatment of DCM.

RDN and mitochondria

Numerous studies have verified that mitochondrial impairment is closely related to cardiac metabolic disorders. Hu et al. found that increased mitochondrial O-GlcNAcylation impaired the activity of respiratory chain enzyme complexes, thus lowering the mitochondrial ATP level and leading to mitochondrial dysfunction[44]. Cole

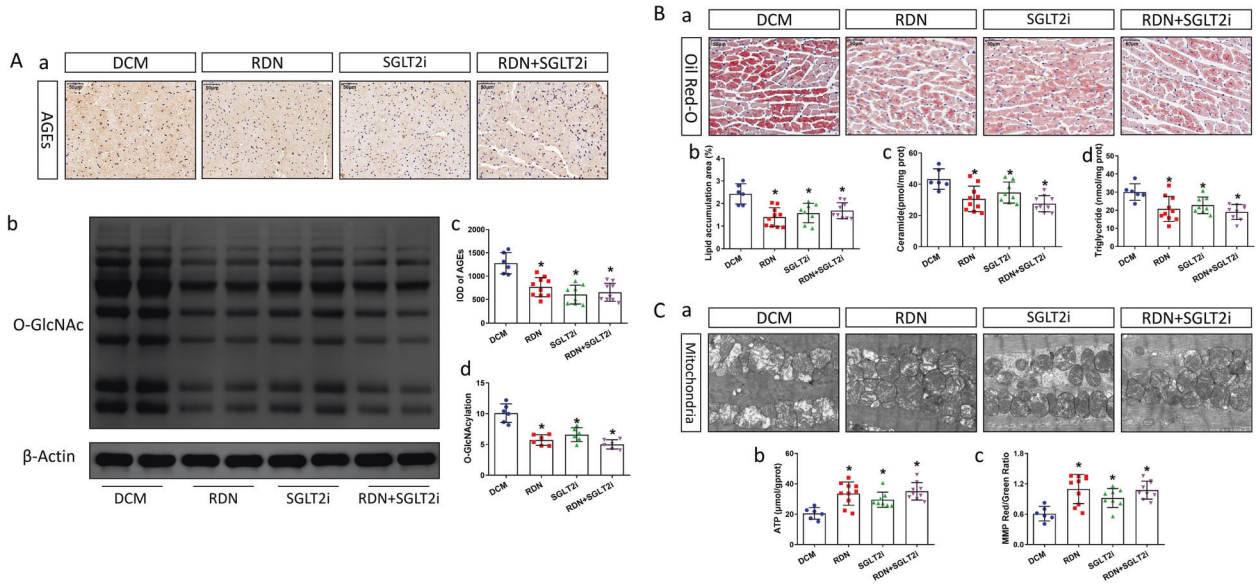

Fig. 6 The protective effects of RDN were mediated by regulation of renal SGLT2 expression. A The combination of RDN and SGLT2i did not further ameliorate glycotoxicity. **a** Representative images of AGEs staining in the myocardium (magnification, ×400) of rats from the four groups. **b** WB analysis of protein levels of O-GlcNAcylation in the hearts. **c** Quantitative analysis of AGEs-positive regions in the heart. **d** The relative levels of O-GlcNAcylation calculated from WB. **B** The combination of RDN and SGLT2i did not further ameliorate lipotoxicity. **a** Representative images of oil red O staining in the hearts (magnification, ×400) of rats from the four groups. **b** Quantitative analysis of lipid accumulation in the heart. **c** ELISA quantification of myocardial ceramide levels. **d** ELISA quantification of myocardial triglyceride levels. **C** The combination of RDN and SGLT2i did not further ameliorate mitochondrial dysfunction. **a** Representative images of mitochondria (magnification, ×7000) of rats from the four groups. (b) ELISA quantification of myocardial ATP levels. **c** The analysis of mitochondrial membrane potential. ($P < 0.05$; $n = 6$, 10, 8, and 9 in the DCM, RDN, SGLT2i and RDN + SGLT2i groups, respectively; five sections were randomly selected per sample.) *$P < 0.05$ vs. the DCM group. AGEs advanced glycation end products.

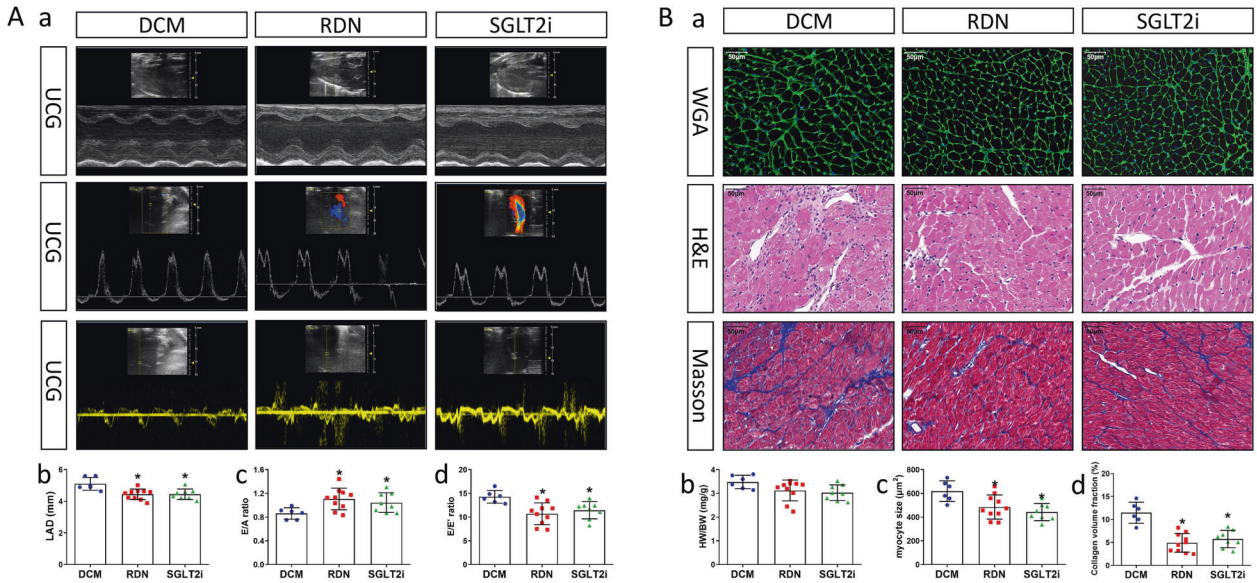

Fig. 7 Comparison between RDN and SGLT2i on the effect of DCM. A RDN was not inferior to SGLT2i in improving cardiac diastolic function. **a** Representative tracings of echocardiography. **b** LAD. **c** E/A ratio. **d** E/E′ ratio. **B** RDN was not inferior to SGLT2i in delaying cardiac pathological remodeling. **a** Representative images of WGA staining (magnification, ×400), HE staining (magnification, ×400) and Masson staining (magnification, ×400) in the hearts. **b** HW/BW ratio. **c** Quantitative analysis of myocyte size calculated from WGA staining. (d) Quantitative analysis of CVF calculated from Masson staining. ($P < 0.05$; $n = 6$, 10, and 8 in the DCM, RDN and SGLT2i groups, respectively; five sections were randomly selected per sample.) *$P < 0.05$ vs. the DCM group. LAD left atrial diameter, WGA wheat germ agglutinin, CVF collagen volume fraction.

et al. observed that lipometabolic disturbances could aggravate respiratory uncoupling by increasing mitochondrial uncoupling protein 3 and mitochondrial thioesterase 1 levels[45]. All these findings indicated that mitochondrial function is tightly regulated by myocardial metabolism. On this basis, damaged mitochondria can further exacerbate disturbances in oxidative stress, mitochondrial dynamics, Ca^{2+} handling and energy metabolism. The synergistic effect of these factors ultimately results in cardiac dysfunction and myocardial remodeling[46]. In our study, we observed that RDN effectively improved mitochondrial

morphology and function. In addition, RDN increased mitochondrial ATP production by restoring the activity of electron respiratory chain enzymes. Together, the findings of the present study confirmed that RDN could ameliorate the glucotoxicity and lipotoxicity of the myocardium under diabetic conditions and that the beneficial effect of RDN on mitochondria may be closely related to the improvement of energy metabolism.

Limitations

Several limitations in the present study should be acknowledged. First, the RDN procedure was performed by phenol ablation to remove the sympathetic nerves. Although this method is widely recognized in small animals, it cannot completely simulate clinical methodology. Therefore, the efficacy of RDN on DCM needs to be further verified in clinical studies. Second, our follow-up time was 13 weeks. Previous studies have confirmed that the DCM model at this stage has typical features of cardiac pathological remodeling and diastolic dysfunction. Therefore, this stage is suitable for investigating the effects of RDN. However, the further accumulation of drugs over time and nerve regeneration after RDN may affect the outcome. Finally, future investigations are required to elucidate the signaling mechanisms underlying RDN-related suppression of renal SGLT2 expression.

CONCLUSIONS

RDN can effectively improve metabolic disturbances and mitochondrial damage in diabetic cardiomyopathy. This protective effect of RDN is mediated by regulation of the expression of SGLT2 in the kidney.

DATA AVAILABILITY

The datasets used and/or analyzed during the current study are available from the corresponding author on reasonable request.

REFERENCES

1. Saeedi, P. et al. Mortality attributable to diabetes in 20–79 years old adults, 2019 estimates: Results from the International Diabetes Federation Diabetes Atlas, 9 (th) edition. *Diabetes Res. Clin. Pract*. **162**, 108086 (2020).
2. Ogurtsova, K. et al. IDF Diabetes Atlas: Global estimates for the prevalence of diabetes for 2015 and 2040. *Diabetes Res. Clin. Pract.* **128**, 40–50 (2017).
3. Zheng, Y., Ley, S. H. & Hu, F. B. Global aetiology and epidemiology of type 2 diabetes mellitus and its complications. *Nat. Rev. Endocrinol.* **14**, 88–98 (2018).
4. Tan, Y. & Zhang, Z. Mechanisms of diabetic cardiomyopathy and potential therapeutic strategies: preclinical and clinical evidence. *Nat. Rev. Cardiol*. **17**, 585–607 (2020).
5. Kenny, H. C. & Abel, E. D. Heart failure in type 2 diabetes mellitus. *Circ. Res.* **124**, 121–141 (2019).
6. Dhalla, N. S. & Shah, A. K. Role of oxidative stress in metabolic and subcellular abnormalities in diabetic cardiomyopathy. *Int. J. Mol. Sci.* **21**, 2413 (2020).
7. Frati, G. et al. An overview of the inflammatory signalling mechanisms in the myocardium underlying the development of diabetic cardiomyopathy. *Cardiovasc Res.* **113**, 378–388 (2017).
8. Nirengi, S., Peres Valgas da Silva, C. & Stanford, K. I. Disruption of energy utilization in diabetic cardiomyopathy; a mini review. *Curr. Opin. Pharmacol.* **54**, 82–90 (2020).
9. van de Weijer, T., Schrauwen-Hinderling, V. B. & Schrauwen, P. Lipotoxicity in type 2 diabetic cardiomyopathy. *Cardiovasc Res*. **92**, 10–18 (2011).
10. Ducheix, S., Magré, J., Cariou, B. & Prieur, X. Chronic O-glcNAcylation and diabetic cardiomyopathy: the bitterness of glucose. *Front. Endocrinol.* **9**, 642 (2018).
11. Pham, T., Loiselle, D., Power, A. & Hickey, A. J. Mitochondrial inefficiencies and anoxic ATP hydrolysis capacities in diabetic rat heart. *Am. J. Physiol. Cell Physiol.* **307**, C499–C507 (2014).
12. Russo, I. & Frangogiannis, N. G. Diabetes-associated cardiac fibrosis: cellular effectors, molecular mechanisms and therapeutic opportunities. *J. Mol. Cell Cardiol.* **90**, 84–93 (2016).
13. Dewanjee, S. et al. Autophagy in the diabetic heart: a potential pharmacotherapeutic target in diabetic cardiomyopathy. *Ageing Res. Rev.* **68**, 101338 (2021).
14. Esler, M. D. et al. Renal sympathetic denervation in patients with treatment-resistant hypertension (The Symplicity HTN-2 Trial): a randomised controlled trial. *Lancet* **376**, 1903–1909 (2010).
15. Sharp, T. E. 3rd et al. Renal denervation prevents heart failure progression via inhibition of the renin-angiotensin system. *J. Am. Coll. Cardiol.* **72**, 2609–2621 (2018).
16. Polhemus, D. J. et al. Renal sympathetic denervation protects the failing heart via inhibition of neprilysin activity in the kidney. *J. Am. Coll. Cardiol.* **70**, 2139–2153 (2017).
17. Mahfoud, F. et al. Effects of renal denervation on kidney function and long-term outcomes: 3-year follow-up from the Global SYMPLICITY registry. *Eur. Heart J.* **40**, 3474–3482 (2019).
18. Bhatt, D. L. et al. A controlled trial of renal denervation for resistant hypertension. *N. Engl. J. Med.* **370**, 1393–1401 (2014).
19. Rafiq, K. et al. Role of the renal sympathetic nerve in renal glucose metabolism during the development of type 2 diabetes in rats. *Diabetologia* **58**, 2885–2898 (2015).
20. Hussein, A. M. et al Comparative study of the effects of GLP1 analog and SGLT2 inhibitor against diabetic cardiomyopathy in type 2 diabetic rats: possible underlying mechanisms. *Biomedicines* **8**, 43 (2020).
21. Arow, M. et al. Sodium-glucose cotransporter 2 inhibitor Dapagliflozin attenuates diabetic cardiomyopathy. *Cardiovasc. Diabetol.* **19**, 7 (2020).
22. Mahfoud, F. et al. Effect of renal sympathetic denervation on glucose metabolism in patients with resistant hypertension: a pilot study. *Circulation* **123**, 1940–1946 (2011).
23. Lee, H. C. et al. The sodium-glucose co-transporter 2 inhibitor empagliflozin attenuates cardiac fibrosis and improves ventricular hemodynamics in hypertensive heart failure rats. *Cardiovasc Diabetol.* **18**, 45 (2019).
24. Jurowich, C. F. et al. Duodenal-jejunal bypass improves glycemia and decreases SGLT1-mediated glucose absorption in rats with streptozotocin-induced type 2 diabetes. *Ann. Surg*. **258**, 89–97 (2013).
25. Zegre Cannon, C., Kissling, G. E., Goulding, D. R., King-Herbert, A. P. & Blankenship-Paris, T. Analgesic effects of tramadol, carprofen or multimodal analgesia in rats undergoing ventral laparotomy. *Lab. Anim.* **40**, 85–93 (2011).
26. Zhang, B. et al. Renal denervation effects on myocardial fibrosis and ventricular arrhythmias in rats with ischemic cardiomyopathy. *Cell Physiol. Biochem.* **46**, 2471–2479 (2018).
27. Wang, L. et al. Decreased autophagy in rat heart induced by anti-β1-adrenergic receptor autoantibodies contributes to the decline in mitochondrial membrane potential. *PLoS One* **8**, e81296 (2013).
28. Shi, W., Wang, Y., Peng, J., Qi, S. & Vitale, N. EPHB6 controls catecholamine biosynthesis by up-regulating tyrosine hydroxylase transcription in adrenal gland chromaffin cells. *J. Biol. Chem*. **294**, 6871–6887 (2019).
29. Parati, G. & Esler, M. The human sympathetic nervous system: its relevance in hypertension and heart failure. *Eur. Heart J.* **33**, 1058–1066 (2012).
30. Zelniker, T. A. & Braunwald, E. Mechanisms of cardiorenal effects of sodium-glucose cotransporter 2 inhibitors: JACC state-of-the-art review. *J. Am. Coll. Cardiol.* **75**, 422–434 (2020).
31. Chong, C. R., Clarke, K. & Levelt, E. Metabolic remodeling in diabetic cardiomyopathy. *Cardiovasc. Res.* **113**, 422–430 (2017).
32. Luiken, J., Nabben, M., Neumann, D. & Glatz, J. F. C. Understanding the distinct subcellular trafficking of CD36 and GLUT4 during the development of myocardial insulin resistance. *Biochim Biophys. Acta. Mol. Basis Dis.* **1866**, 165775 (2020).
33. Park, S. et al. Role of the pyruvate dehydrogenase complex in metabolic remodeling: differential pyruvate dehydrogenase complex functions in metabolism. *Diabetes Metab. J.* **42**, 270–281 (2018).
34. Pepino, M. Y., Kuda, O., Samovski, D. & Abumrad, N. A. Structure-function of CD36 and importance of fatty acid signal transduction in fat metabolism. *Annu. Rev. Nutr.* **34**, 281–303 (2014).
35. Schlaepfer, I. R. & Joshi, M. CPT1A-mediated fat oxidation, mechanisms, and therapeutic potential. *Endocrinology* **161**, 1–14 (2020).
36. Matthews, V. B. et al. Role of the sympathetic nervous system in regulation of the sodium glucose cotransporter 2. *J. Hypertens* **35**, 2059–2068 (2017).
37. Gueguen, C. et al. Empagliflozin modulates renal sympathetic and heart rate baroreflexes in a rabbit model of diabetes. *Diabetologia* **63**, 1424–1434 (2020).
38. Jordan, J. et al. The effect of empagliflozin on muscle sympathetic nerve activity in patients with type II diabetes mellitus. *J. Am. Soc. Hypertens* **11**, 604–612 (2017).
39. Verma, S. et al. Empagliflozin increases cardiac energy production in diabetes: novel translational insights into the heart failure benefits of SGLT2 inhibitors. *JACC Basic Transl. Sci.* **3**, 575–587 (2018).
40. Ramírez, E. et al. Sitagliptin improved glucose assimilation in detriment of fatty-acid utilization in experimental type-II diabetes: role of GLP-1 isoforms in Glut4 receptor trafficking. *Cardiovasc. Diabetol* **17**, 12 (2018).
41. Nakamura, M. & Sadoshima, J. Cardiomyopathy in obesity, insulin resistance and diabetes. *J. Physiol.* **598**, 2977–2993 (2020).

42. Ferrannini, E., Mark, M. & Mayoux, E. CV protection in the EMPA-REG outcome trial: a "Thrifty Substrate" hypothesis. *Diabetes Care* **39**, 1108–1114 (2016).
43. Nakamura, M. & Sadoshima, J. Ketone body can be a fuel substrate for failing heart. *Cardiovasc. Res.* **115**, 1567–1569 (2019).
44. Hu, Y. et al. Increased enzymatic O-GlcNAcylation of mitochondrial proteins impairs mitochondrial function in cardiac myocytes exposed to high glucose. *J. Biol. Chem.* **284**, 547–555 (2009).
45. Cole, M. A. et al. A high fat diet increases mitochondrial fatty acid oxidation and uncoupling to decrease efficiency in rat heart. *Basic Res. Cardiol.* **106**, 447–457 (2011).
46. Bhagani, H. et al. The mitochondria: a target of polyphenols in the treatment of diabetic cardiomyopathy. *Int. J. Mol. Sci.* **21**, 4962 (2020).

AUTHOR CONTRIBUTIONS

J.Y.H. and W.Y.J. performed nearly all the experiments and were the major contributors to the writing of the manuscript. S.G.Z. and Y.T.L. performed the ^{18}F-FDG PET/CT and metabolic cage studies. J.G. and M.C. performed the echocardiographic and electron microscopic studies. J.G. and Y.Y.C. conducted and analyzed the mitochondrial function measurements. Q.J.S. and Z.X.J. were the corresponding authors, and all the experiments were performed under their guidance. All authors read and approved the final paper.

FUNDING INFORMATION

This study was supported by the National Natural Science Foundation of China (No. 81770333, No. 81800350).

COMPETING INTERESTS

The authors declare no competing interests.

ETHICS APPROVAL

All animal experiments in this study were approved by the Ethics Committee of Nanjing Medical University (IACUC-2011003).

ADDITIONAL INFORMATION

Correspondence and requests for materials should be addressed to Zhi-Xin Jiang or Qi-Jun Shan.